Received: 27 March 2023 | Revised: 27 June 2023 | Accepted: 3 August 2023

DOI: 10.1111/iep.12490

ORIGINAL ARTICLE

INTERNATIONAL JOURNAL OF Experimental Pathology WILEY

Inhibition of inflammation and infiltration of M2 macrophages in NSCLC through the ATF3/CSF1 axis: Role of miR-27a-3p

Bin Zhou[1] | **Yan Xu**[2] | **Li Xu**[2] | **Yi Kong**[2] | **Kang Li**[2] | **Bolin Chen**[2] | **Jia Li**[2]

[1]The First Department of Thoracic Surgery, Hunan Cancer Hospital/The Affiliated Cancer Hospital of Xiangya School of Medicine, Central South University, Changsha, China

[2]The Second Department of Thoracic Oncology, Hunan Cancer Hospital/The Affiliated Cancer Hospital of Xiangya School of Medicine, Central South University, Changsha, China

Correspondence
Bolin Chen and Jia Li, The Second Department of Thoracic Oncology, Hunan Cancer Hospital/The Affiliated Cancer Hospital of Xiangya School of Medicine, Central South University, Changsha, China.
Email: chenbolin@hnca.org.cn and lijia@hnca.org.cn

Funding information
Natural Science Foundation of Hunan Province, Grant/Award Number: No.2023JJ30369; The Key Guidance Subject of Health and Health Commission of Hunan Province Scientific Research Program, Grant/Award Number: No.C202303027597

Abstract

Non-small cell lung cancer (NSCLC) imposes a significant economic burden on patients and society due to its low overall cure and survival rates. Tumour-associated macrophages (TAM) affect tumour development and may be a novel therapeutic target for cancer. We collected NSCLC and tumour-adjacent tissue samples. Compared with the tumour-adjacent tissues, the Activation Transcription Factor 3 (ATF3) and Colony Stimulating Factor 1 (CSF-1) were increased in NSCLC tissues. Levels of ATF3 and CSF-1 were identified in different cell lines (HBE, A549, SPC-A-1, NCI-H1299 and NCI-H1795). Overexpression of ATF3 in A549 cells increased the expression of CD68, CD206 and CSF-1. Moreover, levels of CD206, CD163, IL-10 and TGF-β increased when A549 cells were co-cultured with M0 macrophages under the stimulation of CSF-1. Using the starbase online software prediction and dual-luciferase assays, we identified the targeting between miR-27a-3p and ATF3. Levels of ATF3, CSF-1, CD206, CD163, IL-10 and TGF-β decreased in the miR-27a mimics, and the tumour growth was slowed in the miR-27a mimics compared with the mimics NC group. Overall, the study suggested that miR-27a-3p might inhibit the ATF3/CFS1 axis, regulate the M2 polarization of macrophages and ultimately hinder the progress of NSCLC. This research might provide a new therapeutic strategy for NSCLC.

KEYWORDS

ATF3/CFS1 axis, M2 macrophages, miR-27a-3p, NSCLC, TAM

1 | INTRODUCTION

Non-small cell lung cancer (NSCLC) is a critical subtype of lung cancer with very poor prognosis.[1] Cancer treatments such as small-molecule tyrosine kinase inhibitors and immunotherapy have made remarkable progress. However, NSCLC patients still have a poor prognosis.[2]

Researchers believe that the cellular components of the tumour microenvironment (TME) play a crucial role in regulating cancer markers. Among them, tumour-associated macrophages (TAM) affect the anti-inflammatory response and tumour development and are key modulators of the tumour microenvironment.[3] As the tumour progresses, macrophages are actively recruited into the TME and change their functional phenotype in

Bin Zhou and Yan Xu contributed equally to this paper. They are co-first authors.

response to signals generated by tumour cells. Therefore, there is a growing interest in targeting TAM and to explore their role in new treatment strategies for NSCLC.

miRNAs can be involved in gene expression regulation and cellular process networks. miRNA and TME are linked to the development of cancer features. Therefore, targeting miRNA-mediated regulation of TME holds potential as a therapeutic strategy.[4] Macrophages are important immune cells and play an indispensable role in primordial and acquired immunity.[5] M1 macrophages are known to produce pro-inflammatory cytokines, antibacterial and anticancer activities. On the other hand, M2 macrophages are associated with immunosuppression, tumorigenesis and parasite elimination.[6] A number of miRNAs have been shown to induce macrophage-mediated polarization by targeting various transcription factors and adaptor proteins.[7] For instance, hypoxia pre-attack-mediated extracellular vesicles have been found to promote NSCLC cell growth and M2 macrophage polarization through miR-21-5p delivery.[8] Additionally, reduced levels of miR-27a-3p have been reported in NSCLC.[9] Regulation of miR-27a-3p can affect the cell activity and erastin sensitivity of NSCLC cells.[9,10] Furthermore, miR-27a-3p has been linked to M2 macrophage polarization in glioblastoma (GBM).[11] Taking these factors into consideration, we focus on miR-27a-3p and macrophage polarization in NSCLC.

Activated transcription factor 3 (ATF3) is a crucial player in regulating metabolism, immunity and tumorigenesis.[12] In NSCLC and melanoma studies, the ATF3-PD-L1 axis is involved in the immune regulation of tumour cells.[13] In addition, colony-stimulating factor 1(CSF-1) is often upregulated in various cancers. TAM is a promising drug target for cancer.[14] Moreover, CFS1 secreted by tumour cells could promote the differentiation of M0 macrophages into M2-type macrophages.[15] Interestingly, miR-27a-3p has been shown to decrease calcium deposition via ATF3.[16] However, the specific role of miR-27a-3p, ATF3 and CSF-1 in NSCLC is yet to be fully understood.

In brief, we assumed that miR-27a-3p might affect NSCLC development via macrophage polarization. In the study, we identified the expression of ATF3 and CSF-1 in clinical samples. Further, we verified our hypothesis through cell and animal experiments.

2 | METHODS

2.1 | Clinical sample collection

Nine Tumour-Adjacent tissue cases and nine cases of NSCLC tissue were collected from Cancer Hospital. All patients were selected in accordance with the guidelines of the World Health Organization and the International Association for the Study of Lung Cancer, and patient informed consent was obtained. The study was approved by the Ethics Committee of Hunan Cancer Hospital (No. SBQLL-2021-215).

2.2 | Cell culture

Human bronchial epithelial cells (HBE) and lung cancer epithelial cells (NCI-H1299 and NCI-H1975) were acquired from ATCC. Human lung adenocarcinoma cells (SPC-A-1) and macrophages (THP-1) were purchased from Shanghai EK-Bioscience. A549 cells were purchased from HonorGene. All cells were cultured in RPMI-1640 medium (PM150110; Thermofly) supplemented with 10% foetal bovine serum and 1% penicillin–streptomycin solution (PB180120; Thermofly) was added to prevent bacterial contamination. The culture was maintained at 37°C, with 95% air and 5% CO_2. M0 macrophages were induced from THP-1 by the Phorbol 12-myristate 13-acetate (PMA).

2.3 | Cell transfection

To study the effects of ATF3 and miR-27a, we manipulated the levels of these factors utilizing packaged lentiviruses (including oe-ATF3, oe-NC, sh-ATF3 and sh-NC), miR-27a mimics and inhibitors, as well as mimics and inhibitors of negative control (mimics NC and NC inhibitor). These lentiviruses and reagents were obtained from Shanghai GenePharma. A549 cells were cultured in a medium containing Lipofectamine 2000 (11668500; Invitrogen) for 6 h, and an appropriate amount of plasmids was added. Polybren was used as a co-transfection agent when lentivirus was transfected into A549 cells. Forty eight hour after transfection, cells were used for further detection. Cells in the NC group were accompanied by transfection of oe-NC and sh-NC, while untreated cells were included in the Blank group.

2.4 | Transwell co-culture assay

Before the co-culture assay, A549 cells were divided into the M0 and M0-CSF1 groups. The 25 ng/μL CSF1[15] was incubated with the A549 cells in the M0-CSF1 group. Macrophages were then collected, and phenotypic changes were identified via flow cytometry.

In order to investigate the impact of ATF3 in A549 cells on the polarization of macrophages, we designed the following experimental groups: Blank, NC, oe-ATF3,

oe-ATF3 + α-CSF-1 Ab, sh-ATF3 and sh-ATF3 + CSF. Indirect co-culture of A549 and macrophages was performed using a 3.0 μm transwell (353,492; Corning).[15] In the presence of PMA, M0 macrophages were inoculated in the bottom of the transwell, and A549 cells were inoculated into the upper pore. The 25 ng/μL CSF1 and 1.0 μg/mL anti-α-CSF-1 were added into the co-culture system.[15] Macrophage cell types were determined through flow cytometry analysis.

To further analyse the effect of miR-27a and ATF3 on macrophage polarization in A549 cells, the following groups were set: Blank, mimics NC, miR-27a mimics and miR-27a mimics + oe-ATF3. Stable A549 cells (mimics NC, miR-27a mimics, miR-27a mimics + oe-ATF3) were constructed, and A549 cells were co-cultured with macrophages. Cells in the blank group were treated as previously described. Flow cytometry was used to identify macrophage cell types.

2.5 | Macrophage chemotaxis assay

To analyse the effect of miR-27a and ATF3 in A549 cells on macrophage chemotaxis, a co-culture system of A549 cells and macrophages was constructed as described previously. A549 cells stably transfected with mimics NC, miR-27a mimics and oe-ATF3 were placed in the lower chamber of transwell, and macrophages were placed in the upper chamber. After 48 h, the upper chamber was removed and fixed with 4% paraformaldehyde for 20 min. The cells were stained with 0.1% crystal violet for 5 min. After washing, the samples were observed under a microscope and photographed.

2.6 | Xenograft mouse model

Thirty male BALB/c nude mice (4 weeks) were ordered from Hunan SJA. The mice were divided into the NC, oe-ATF3, sh-ATF3, mimics NC and miR-27a mimics groups ($n = 6$ for each group). The cells were injected subcutaneously into the armpit of the anterior left limb of nude mice at the rate of 3×10^6/100 μL/piece. The cells were transfected with oe-ATF3, sh-ATF3, oe-NC and sh-NC and then inoculated into mice. After transfection of miR-27a-3p mimics and mimics NCs into A549 cells, the cells were inoculated into mice. The tumours were measured and observed twice a week. Twenty eight days after transfection, 150 mg/kg barbiturate was injected intraperitoneally for euthanasia. The tumours were photographed and further detected. All animal experiments were approved by the Ethics Committee of Hunan Cancer Hospital (NO. SBQLL-2021-215).

2.7 | Reverse transcription-quantitative PCR (RT-qPCR)

Total mRNA was extracted with trizol. The primers of genes were biosynthesized by Beijing Tsingke Biotechnology Co., Ltd. The mRNA reverse transcription kit (CW2569) and miRNA reverse transcription kit (CW2141) were used. RT-qPCR was conducted in a fluorescence PCR instrument (PIKOREAL96, Thermo). β-actin and U6 were applied as internal references. The mRNA levels were calculated via the $2^{-\Delta\Delta C_t}$. The primer sequences used were as follows:

ATF3 forward: 5′-AAAACCAGGATGCCCACCGTT-3′, reverse: 5′-CCACATCCCCTACGAGTGACA-3′.

CSF1 forward: 5′-AAGTTTGCCTGGGTCCTCTC-3′, reverse: 5′-AGACCAACAACAGCAGGGAG-3′.

CD206forward:5′-TATGCCAGACACGATCCGACCC-3′, reverse: 5′-AGTATGTCTCCGCTTCATGCCAT-3′.

IL-10 forward: 5′-ACCTGCCTAACATGCTTCGAGA-3′, reverse: 5′-CTCAGCTTGGGGCATCACCT-3′.

TGF-β forward: 5′-AGCAACAATTCCTGGCGATAC CTC-3′, reverse: 5′-CAATTTCCCCTCCACGGCTCA-3′.

CD163 forward: 5′-AAAAGAATCCCGCATTTGGC AGT-3′, reverse: 5′-GCCAACAGTGCCCCAAGCTC-3′.

miR-27a-3p forward: 5′-TTCACAGTGGCTAAGTTC CGC-3′, reverse: 5′-GCTGTCAACGATACGCTACGTAA-3′.

U6 forward: 5′-CTCGCTTCGGCAGCACA-3′, reverse: 5′-AACGCTTCACGAATTTGCGT-3′.

β-actinforward:5′-ACCCTGAAGTACCCCATCGAG-3′, reverse: 5′-AGCACAGCCTGGATAGCAAC-3′.

2.8 | Western blot (WB)

RIPA lysates were applied to extract total proteins. Proteins of target molecular weight were screened by the SDS-PAGE. The target proteins on the gel were then transferred to the nitrocellulose membrane. After sealing in 5% skim milk powder, the membrane was incubated with primary antibodies ATF3 (ab254268, 1:1000; Abcam), CSF-1 (ab233387, 1:1000; Abcam) and β-actin (66009-1-Ig, 1:1000; Proteintech) and secondary antibodies for 90 min. The proteins were visualized by SuperECL Plus luminescence solution (AWB0005; Abiowell). β-actin was used as the housekeeping protein.

2.9 | Immunohistochemistry (IHC)

The tissue samples were sliced into 2 μm thick sections. After being placed at 60°C for 12 h, the xylene and gradient-concentration ethanol were used for dewaxing and rehydrating. The antigen repair was performed, and 1% periodate acid was used to inactivate the endogenous enzymes. Primary antibody CD68 (ab955; Abcam) was

incubated with the sections overnight at a 1:200 dilution. After incubation of secondary antibodies, sections were incubated with DAB and haematoxylin solution to develop colour. Sections were sealed with neutral gum. The images were viewed using a light microscope and analysed using Image-pro-plus software.

2.10 | Immunofluorescence (IF)

Sections were dewaxed, rehydrated and heated. Then the sections were treated with sodium borohydride solution, ethanol solution and Sudan black for 5 min, 1 min and 15 min, respectively. After rinsing with running water, the sections were immersed in 5% BSA for 60 min. Primary antibodies, including CD206 (60143-1-Ig, 1:50; Proteintech), ATF3 (ab254268, 1:50; Abcam) and CSF-1(25949-1-AP, 1:50; Proteintech), were incubated with sections. Secondary antibodies were used to treat the sections. DAPI working solution was adopted to stain the nuclei. The sections were closed with buffer glycerin and observed with a fluorescence microscope.

2.11 | Enzyme-linked immunosorbent assay (ELISA)

The levels of CSF-1 in cell supernatant were analysed using the human Macrophage Colony-Stimulating Factor (M-CSF) ELISA kit (CSB-E04658h; CUSABIO). All operations were performed as instructed. After the reaction stopped, a microplate reader was operated to examine the absorbance (450 nm).

2.12 | Flow cytometry

10^6/100 μL cells were taken into the 1.5 mL EP tube. After centrifuging, cells were stained with 0.125 μg CD68 (11-0689-42; eBiosciences) and 0.25 μg CD163 (12-1639-42; eBiosciences). Then cells were washed and resuspended with 150 μL PBS. Finally, cell suspensions were examined by flow cytometry (A00-1-1102; Beckman).

2.13 | Chromatin immunoprecipitation coupled with qPCR (ChIP-qPCR)

ChIP-qPCR was performed as described previously.[17] First, ChIP was performed according to the ChIP kit (ab500; Abcam) manufacturer's instructions. After cells were fixed with formaldehyde for 10 min, glycine was added to quench the formaldehyde. After adding the protease inhibitor and buffer mixture, the cells were disrupted by sonication (ultrasonic 4 s, gap 6 s, total time 60 s, power 20%). Chromatin was incubated with anti-ATF3 (ab254268; Abcam) and rotated overnight at 4°C. The antibody-chromatin complexes were mixed with the Bead at 4°C for 60 min for immunoprecipitation. After extraction of immunoprecipitated DNA, qPCR was performed. The ChIP-qPCR primer was CSF-1 forward: 5′-AGCAA ATGAATGGCAGAG-3′, reverse: 5′-ATGGGTTCTAA AGCAATGAC-3′.

2.14 | Dual-luciferase assay

The pHG-miRTarget- ATF3 and pHG-miRTarget- ATF3 MUT were purchased from Changsha Honorgene. Dual-luciferase® Reporter Assay System (E1910) was obtained from Promega. All operation steps strictly follow the instructions. The fluorescence signal intensity was measured using Promega's GloMax 20/20 chemiluminescence detector.

2.15 | Statistical analysis

Statistical analyses were performed via GraphPad Prism 8.0.1. Data were presented as mean ± standard deviation and analysed by unpaired Student's *t*-test, one-way ANOVA and two-way ANOVA. $p < .05$ was considered statistically significant.

3 | RESULTS

3.1 | ATF3 and CSF-1 levels increased in NSCLC

To investigate the changes of ATF3 and CSF-1 in NSCLC, we examined the expression of ATF3 and CSF-1 at transcription and translation levels. As shown in Figure 1A,B, compared with the Tumour-adjacent tissue, protein and mRNA expressions of ATF3 and CSF-1 increased in NSCLC tissue. The protein and mRNA levels of ATF3 and CSF-1 increased in A549, SPC-A-1, NCI-H1299 and NCI-H1975 cells compared with HBE. Among them, A549 cells had the highest protein and mRNA expression levels of ATF3 and CSF-1 (Figure 1C,D). Pearson analysis showed that ATF3 was positively correlated with CSF-1 (Figure 1E, $r = .7935$, $p < .0001$). In other words, the expression of ATF3 and CSF-1 was increased.

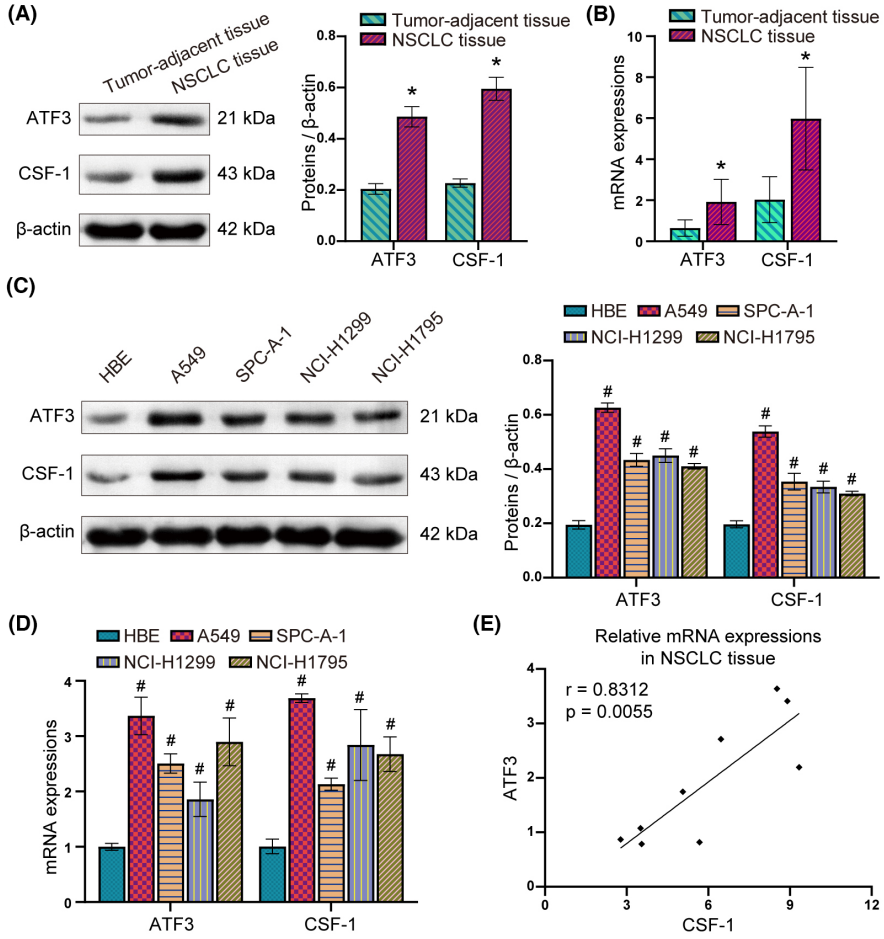

FIGURE 1 ATF3 and CSF-1 are highly expressed in NSCLC. (A, B) The ATF3 and CSF-1 levels in the tissues were detected by WB and RT-qPCR. $^{*}p < .05$ versus the Tumour-adjacent tissue ($n = 9$ for each group), unpaired t-test. (C, D) ATF3 and CSF-1 levels in the Cells were detected by WB and RT-qPCR. $^{\#}p < .05$ versus the HBE ($n = 3$ for each group), one-way ANOVA. (E) The correlation between ATF3 and CSF-1 using Pearson correlation analysis.

3.2 | ATF3 promotes M2 macrophage infiltration in xenograft tumours

To understand the impact of ATF3 on the development of NSCLC, we conducted experiments in which we overexpressed and knocked down ATF3 in A549 cells. We examined ATF3 expression in A549 cells at translation and transcription levels. According to Figure 2A and B, A549 cells with ATF3 overexpression and knockdown were successfully obtained. To further explore the impact of ATF3 on tumour development, we transplanted these cells into mice. Figure 2C shows the tumour of mice 28 days after transplantation. Compared with the NC, the volume and weight of tumours increased in the oe-ATF3 and decreased in the sh-ATF3 groups, suggesting that ATF3 could promote tumour development. IHC, IF and RT-qPCR results reflected that the CD68 and CD206 increased in the oe-ATF3 and reduced in the sh-ATF3 groups (Figure 2D–F). CD68 is a major biomarker for quantifying the total number of TAM. The transmembrane receptor CD206 is a biomarker for M2 macrophages.[18] These indicated that ATF3 could promote NSCLC development by increasing the infiltration of M2 macrophages in tumours.

3.3 | ATF3 may promote macrophage M0–M2 conversion by regulating CSF-1

Next, we wonder whether the promoting effect of ATF3 on M2 macrophage infiltration was related to CSF-1. Our findings revealed that the expression of CSF-1 in A549 cells was upregulated in the oe-ATF3 group and downregulated in the sh-ATF3 group, as shown in Figure 3A–C. These results reflected that ATF3 could activate the expression of CSF-1. Furthermore, we used the JASPAR software online (http://jaspar.genereg.net/) to predict the ATF and CSF-1 potential binding sites motif, as shown in Figure S1A. However, ChIP-qPCR analysis showed that the binding between ATF and CSF-1 was negative (Figure S1B). This finding suggested that ATF3 might regulate CSF-1 expression via alternative pathways.

The $CD68^{+}CD163^{+}$ cells in the M0-CSF increased. This demonstrated that CSF-1 might promote the conversion of macrophages M0–M2 (Figure 3D). CD206, CD163, TGF-β and IL-10 levels were higher in the M0-CSF than in the M0 groups (Figure 3E). CD163 and CD206 are macrophage activation markers and are upregulated in the inflammatory response.[19] Our results suggested that CSF-1 might promote inflammation in tumour cells. Furthermore, our findings

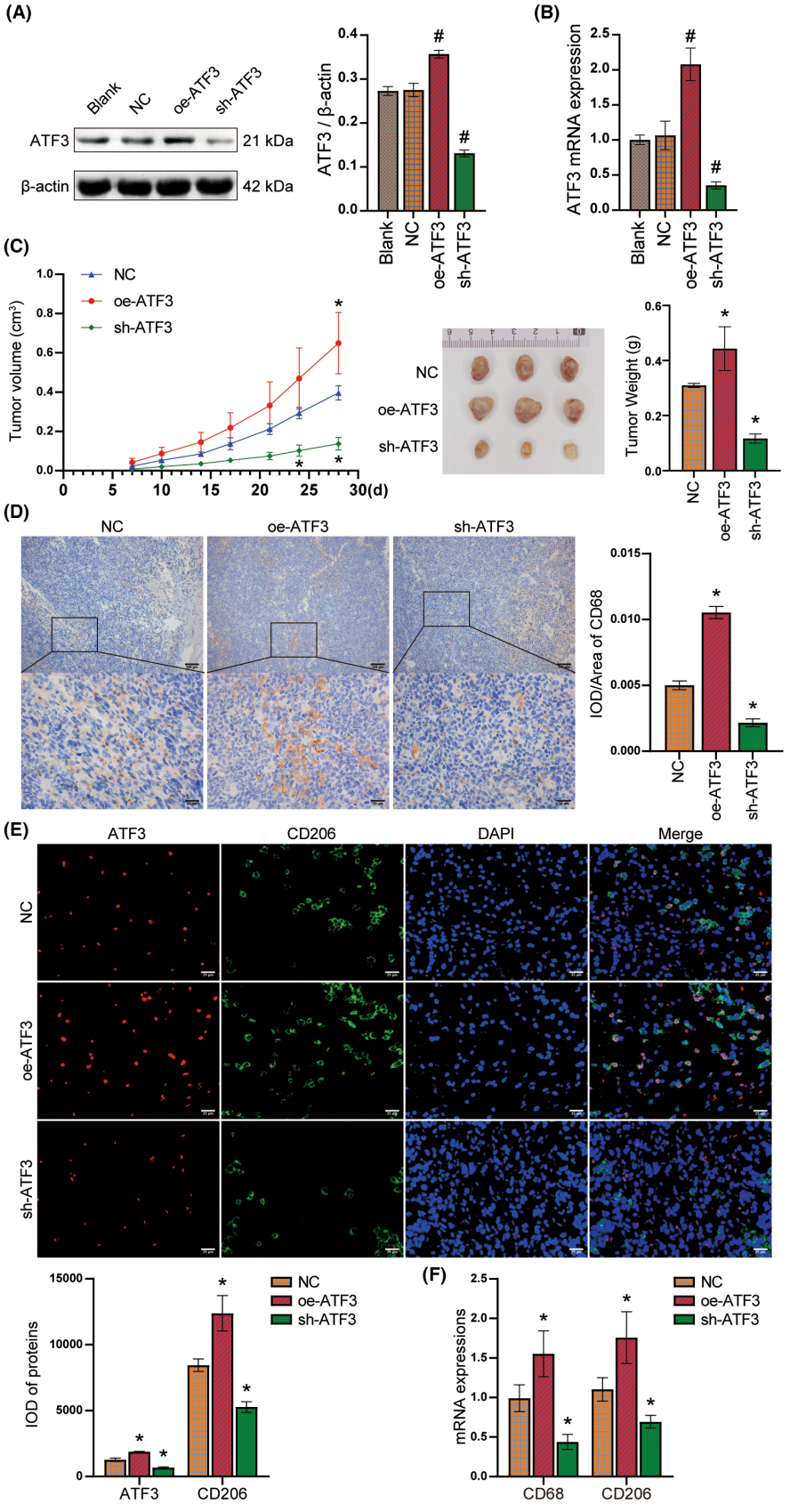

FIGURE 2 ATF3 could promote M2 macrophage infiltration in xenograft tumours. (A) WB was utilized to monitor the expression of ATF3. (B) Levels of ATF3 were captured by RT-qPCR. $^{\#}p < .05$ versus the NC ($n = 3$ for each group), one-way ANOVA. (C) The volume and weight of tumour tissues. (D) IHC was conducted to test ATF3 expression in the tumour. (E) IF was adopted to analyse the ATF3 and CD206 expression. (F) The mRNA levels of CD68 and CD206 in tumour tissues. $^{*}p < .05$ versus the NC ($n = 6$ for each group), one-way ANOVA and two-way ANOVA. Magnification = 100/400 times. Scale bar = 100/25 μm.

showed a significant increase in $CD68^{+}CD163^{+}$ cells in the oe-ATF3 group; this increase, however, was reversed by treatment with α-CSF-1 antibody. The $CD68^{+}CD163^{+}$ cells increased in the sh-ATF3 + CSF group compared with the sh-ATF3. Our results indicated that ATF3 might promote the infiltration of M2 macrophages through CSF-1.

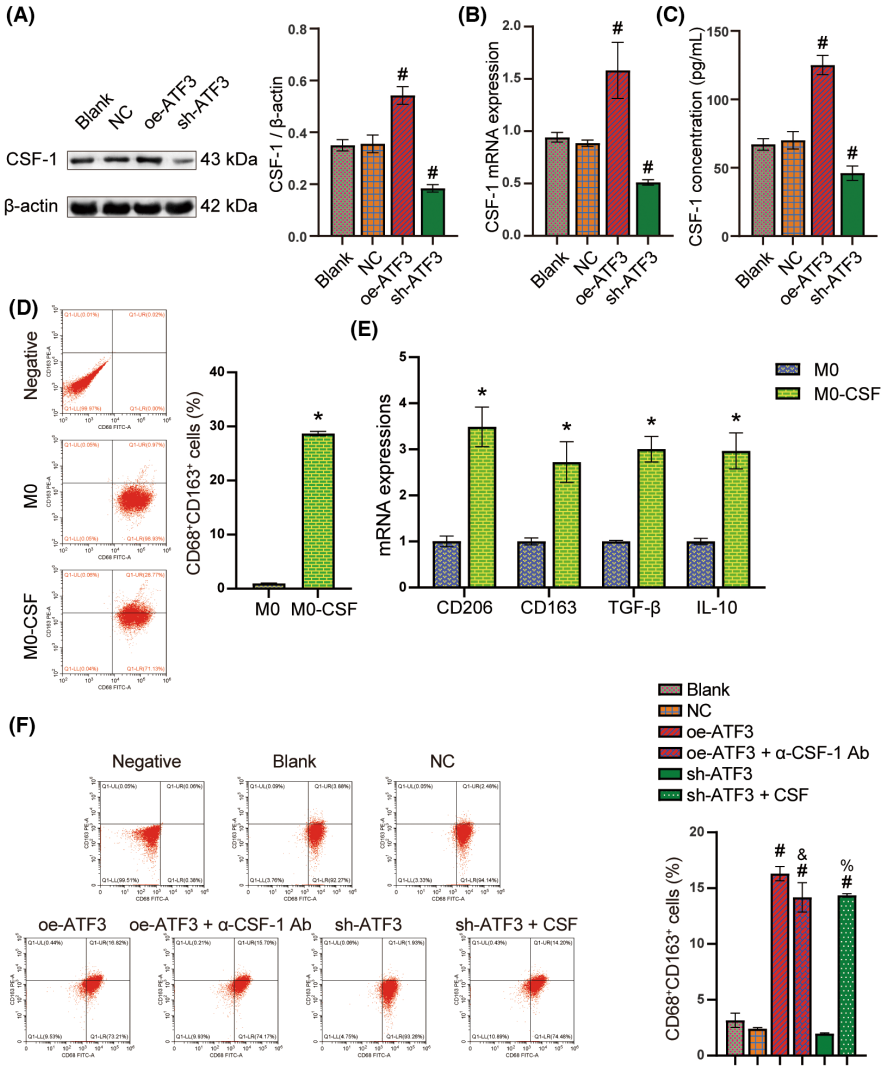

FIGURE 3 ATF3 promotes macrophage M0–M2 conversion by regulating CSF-1. CSF-1 levels were analysed via WB (A), RT-qPCR (B) and ELISA (C) $^{\#}p < .05$ versus the NC ($n = 3$ for each group), one-way ANOVA. (D) Flow cytometry was performed to measure the radio of $CD68^{+}CD163^{+}$ cells. (E) CD206, CD163, TGF-β and IL-10 mRNA levels were tested. $^{*}p < .05$ versus the M0 ($n = 3$ for each group), unpaired *t*-test. (F) The radio of $CD68^{+}CD163^{+}$ cells was measured. $^{\#}p < .05$ versus the NC, $^{\&}p < .05$ versus the oe-ATF3, and $^{\%}p < .05$ versus the sh-ATF3 ($n = 3$ for each group), one-way ANOVA.

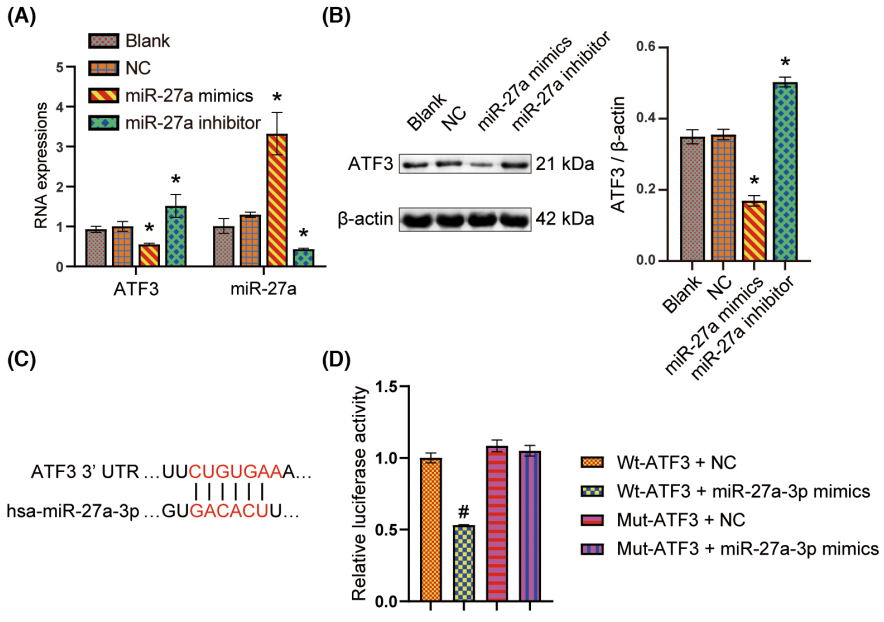

FIGURE 4 miR-27a-3p regulates ATF3 levels in NSCLC. (A) miR-27a-3p and ATF3 mRNA expression were detected. (B) The protein levels of ATF3 were analysed by WB. $^{*}p < .05$ versus the NC ($n = 3$ for each group), one-way ANOVA. (C) The binding site between miR-27a-3p and ATF3 by the starbase. (D) The binding site was identified using dual-luciferase assay. $^{\#}p < .05$ versus the Wt-ATF3 + NC, one-way ANOVA.

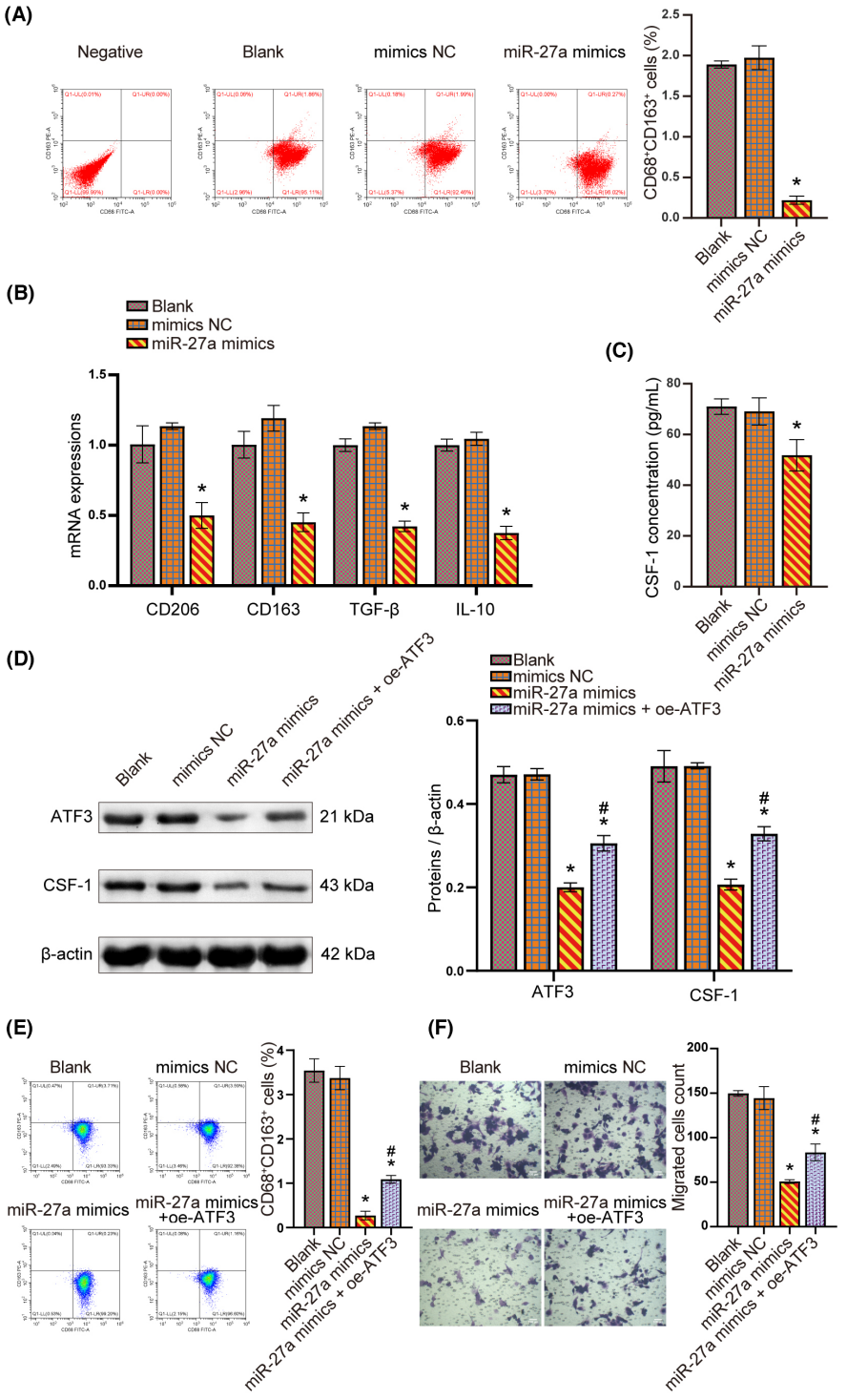

FIGURE 5 Overexpression of miR-27a-3p inhibits macrophage M2 transformation by regulating the ATF3/CSF-1 pathway. (A) The radio of $CD68^+CD163^+$ cells was analysed. (B) RT-qPCR was conducted to test CD206, CD163, TGF-β and IL-10. (C) The concentration of CSF-1 was calculated by ELISA. (D) WB was utilized to analyse the proteins ATF3 and CSF-1. (E) The radio of $CD68^+CD163^+$ cells. (F) Macrophage migration assays. $^*p < .05$ versus the mimics NC and $^{\#}p < .05$ versus the miR-27a mimics ($n = 3$ for each group), one-way ANOVA.

3.4 | miR-27a-3p regulates the ATF3 levels in NSCLC

To explore the regulatory effect of miR-27a-3p on ATF3 in NSCLC, we established cells overexpressing and downregulating miR-27a-3p. As seen in Figure 4A,B, miR-27a-3p was successfully overexpressed and knocked down. The levels of ATF3 in the miR-27a mimics group decreased, while that increased in the miR-27a-3p inhibitor. These results indirectly indicated that miR-27a-3p could suppress the ATF3 levels. However, whether miR-27a-3p interacted directly with ATF3 was unknown. The starbase (http://www.targetscan.org/) forecasted that miR-27a-3p and the gene ATF3 have binding sites (Figure 4C). Dual-luciferase reporter assay was performed, and showed that miR-27a-3p could target ATF3 (Figure 4D). In other words, miR-27a-3p could directly regulate ATF3 levels in NSCLC.

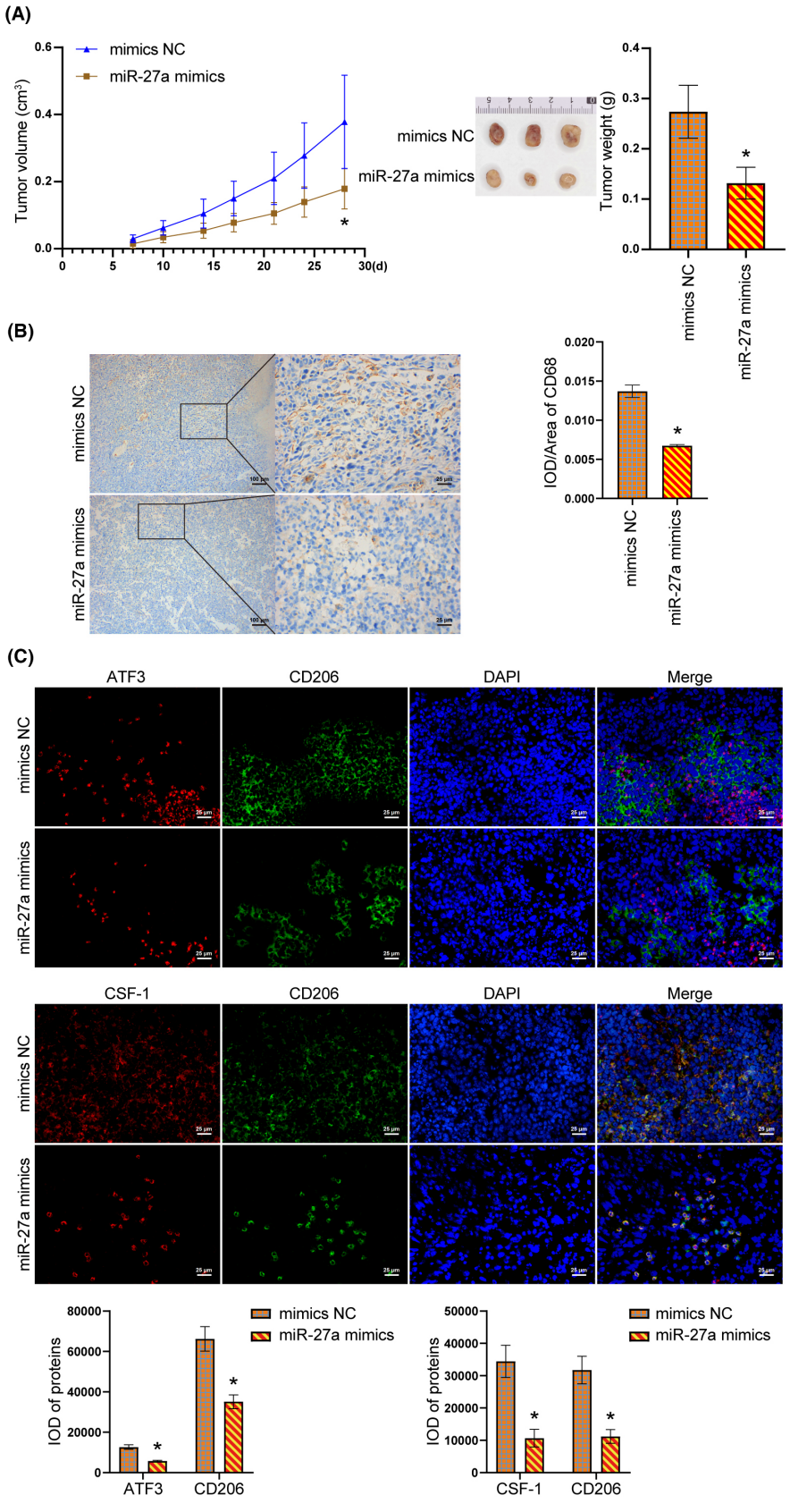

FIGURE 6 miR-27a-3p inhibits macrophage M2 transformation by regulating the ATF3/CSF-1 pathway in vivo. (A) The volume and weight of the tumour. *$p < .05$ versus the mimics NC ($n = 6$ for each group), unpaired t-test and two-way ANOVA. (B) IHC was applied to capture the CD68 cells. (C) IF was utilized to observe the distribution of ATF3, CD206 and CSF-1. *$p < .05$ versus the mimics NC ($n = 6$ for each group), unpaired t-test. Magnification = 100/400 times. Scale bar = 100/25 μm.

3.5 | Overexpression of miR-27a-3p inhibits macrophage M2 transformation by regulating the ATF3/CSF-1 pathway

Finally, the role of miR-27a-3p was further explored. Flow cytometry showed that $CD68^+CD163^+$ cells decreased in the miR-27a mimics group, compared to the mimics NC (Figure 5A). Simultaneously, the levels of CD206, CD163, TGF-β and IL-10 decreased in the miR-27a mimics (Figure 5B). Additionally, a reduction in the concentration of CSF-1 was observed in the miR-27a mimics (Figure 5C). Further, we conducted a rescue experiment. Compared with the mimics NC, the ATF3 and CSF-1 levels decreased in the miR-27a mimics group. However, oe-ATF3 reversed the inhibition of miR-27a mimics on ATF3 and CSF-1 expression and $CD68^+CD163^+$ cells (Figure 5D,E). Macrophage migration assay showed that oe-ATF3 could reverse the inhibitory effect of miR-27a mimics on the migration of $CD68^+CD163^+$ cells (Figure 5F). These hinted that miR-27a-3p might inhibit the transformation of macrophages from M0 to M2 by regulating the ATF3/CSF-1 pathway in cell experiments.

Furthermore, we conducted in vivo experiments to validate our findings. As shown in Figure 6A, the volume and quality of tumours in mice in the miR-27a mimics decreased compared to the mimics NC groups. IHC results revealed that the rate of CD68 cells in tumour tissues decreased in the miR-27a mimics (Figure 6B). IF results demonstrated that CSF-1, ATF3 and CD206 in tumour tissues of the miR-27a mimics decreased (Figure 6C). Therefore, the results validated that miR-27a-3p overexpression in vivo inhibited macrophage transformation from M0 to M2 by regulating the ATF3/CSF-1 pathway.

4 | DISCUSSION

Firstly, we conducted a comparison of the ATF3 and CSF-1 levels between normal and NSCLC samples. Results demonstrated that the ATF3 and CSF-1 expression in NSCLC increased in both clinical tissue and cell samples. Similarly, higher ATF3 expression has been found in breast cancer cells, contributing to radiation resistance in breast cancer.[20] In tumours, ATF3 is known to target multiple signals related to glucose metabolism, immune reactivity and tumorigenesis in tumours.[12] Additionally, CSF-1 produced by tumour cells restricted the migration of TAM to the tumour, and treatment with CSF-1-receptor inhibitors blocked tumour granulocyte infiltration and showed a strong anti-tumour effect.[21] Consistent with other cancers, high expression of ATF3 and CSF-1 might be essential for NSLC development.

After performing an overexpression of ATF3 or CSF-1 in A549 cells, we discovered that ATF3 and CSF-1 had the ability to promote tumour development by regulating macrophage M2 polarization. Earlier studies have shown that ATF3 promoted macrophage migration and M2 polarization through the Wnt/β-catenin pathway.[22] CSF-1 signal could regulate macrophage differentiation through CSF-1 receptors.[23] Similarly, Oct4 promotes the polarization of M2 macrophages by upregulating CSF-1 of lung cancer macrophages.[24] In hepatocellular carcinoma, blocking osteopontin can prevent TAM by blocking CSF-1/CSF1R, a move that can enhance the effectiveness of immune checkpoint inhibitors in HCC treatment.[25] Moreover, our results revealed that ATF3 positively regulated CSF-1 expression. A dorsal root ganglion neurons study revealed that CSF-1 induction was reduced when the ATF3 gene was knocked out from sensory neurons.[26] ATF3 promotes CSF-1 expression and is involved in accumulating macrophages in synovium and pain signalling in dorsal horn macrophages in arthritis.[27] Consequently, in this research, ATF3 might promote the development of NSCLC via CSF-1 and the macrophage M2 polarization.

Our results validated that miR-27a-3p inhibited ATF3 expression. In more detail, miR-27a-3p could target and bind the gene ATF3. Similarly, miR-27a-3p plays a major role in osteogenic differentiation by targeting ATF3.[28] In vascular calcification, miR-27a-3p targets ATF3 to reduce calcium deposition.[16] In other words, miR-27a-3p can target the ATF3/CSF-1 pathway. miR-27a-3p down-regulated the genes ATF3 and CSF-1 and inhibited macrophage M2 polarization and tumour growth in our study. In contrast, miR-27a-3p in glioma could promote the polarization of M2 macrophages through EZH1/KDM3A/CTGF axis.[11] This was not consistent with our results that miR-27a-3p inhibited M2-type macrophage polarization by targeting the ATF3/CSF-1 pathway. miR-27a-3p, which is highly expressed in tuberculosis, can induce M1 macrophage differentiation and inhibit M2 macrophage differentiation by targeting vitamin D receptor.[29] We hypothesized that the effect of miR-27a-3p on macrophage polarization may be related to its regulatory mechanism under different pathological conditions. miRNAs act in almost all aspects of cancer biology.[30] Molecularly distinct tumours can be analysed by specific miRNA for cancer diagnosis, prognosis and treatment.[31] miR-498 inhibits M2 polarization of TAM by MDM2/ATF3.[32] miR-149 inhibits metastasis in breast cancer cells by limiting CSF-1-dependent recruitment and M2 polarization of macrophages.[33] In other words, our experiments revealed that miR-27a-3p targets the ATF3/CSF-1 pathway to limit the development of NSCLS.

Overall, this study revealed that miR-27a-3p plays a critical role in regulating the M2 macrophage ratio by inhibiting the ATF3/CSF-1 pathway, ultimately hindering

the progression of NSCLC. These findings have expanded our understanding of the underlying mechanisms of NSCLC and provided new strategies for NSCLC. However, this study also has many shortcomings. Due to the limitation of funds, we failed to explain the mechanism of the ATF3 regulation of CSF-1. In future work, we will conduct a chromatin immunoprecipitation assay to verify whether ATF3 is involved in CSF-1 promoter enrichment. Additionally, the relationship between miR-27a and M1 macrophage polarization still needs to be further studied, and numerous clinical trials are still needed before miR-27a-3p can be used to treat NSCLC.

AUTHOR CONTRIBUTIONS

Bin Zhou and Yan Xu contributed to conceptualization, data curation, investigation, methodology, validation and writing of the original draft. Li Xu, Yi Kong and Kang Li contributed to conceptualization, formal analysis, investigation, software and validation. Bolin Chen and Jia Li designed the study, performed the research, analysed data and wrote the paper. All authors read and approved the final manuscript.

ACKNOWLEDGEMENTS

None.

FUNDING INFORMATION

This work was supported by the Natural Science Foundation of Hunan Province (No. 2023JJ30369), and the Key Guidance Subject of Scientific Research Program of Hunan Health Commission (No. C202303027597).

CONFLICT OF INTEREST STATEMENT

The authors declare that there are no conflicts of interest.

ORCID

Bolin Chen https://orcid.org/0000-0002-4956-2675

REFERENCES

1. Zhang J, Li H, Wu Q, et al. Tumoral NOX4 recruits M2 tumor-associated macrophages via ROS/PI3K signaling-dependent various cytokine production to promote NSCLC growth. *Redox Biol*. 2019;22:101116. doi:10.1016/j.redox.2019.101116
2. Herbst RS, Morgensztern D, Boshoff C. The biology and management of non-small cell lung cancer. *Nature*. 2018;553(7689):446-454. doi:10.1038/nature25183
3. Chanmee T, Ontong P, Konno K, Itano N. Tumor-associated macrophages as major players in the tumor microenvironment. *Cancers (Basel)*. 2014;6(3):1670-1690. doi:10.3390/cancers6031670
4. Lee SS, Cheah YK. The interplay between MicroRNAs and cellular components of tumour microenvironment (TME) on non-small-cell lung cancer (NSCLC) progression. *J Immunol Res*. 2019;2019:3046379. doi:10.1155/2019/3046379
5. Arora S, Dev K, Agarwal B, Das P, Syed MA. Macrophages: their role, activation and polarization in pulmonary diseases. *Immunobiology*. 2018;223(4–5):383-396. doi:10.1016/j.imbio.2017.11.001
6. Wang N, Liang H, Zen K. Molecular mechanisms that influence the macrophage m1–m2 polarization balance. *Front Immunol*. 2014;5:614. doi:10.3389/fimmu.2014.00614
7. Essandoh K, Li Y, Huo J, Fan GC. MiRNA-mediated macrophage polarization and its potential role in the regulation of inflammatory response. *Shock*. 2016;46(2):122-131. doi:10.1097/shk.0000000000000604
8. Ren W, Hou J, Yang C, et al. Extracellular vesicles secreted by hypoxia pre-challenged mesenchymal stem cells promote non-small cell lung cancer cell growth and mobility as well as macrophage M2 polarization via miR-21-5p delivery. *J Exp Clin Cancer Res*. 2019;38(1):62. doi:10.1186/s13046-019-1027-0
9. Liang Q, Zhang H. MAP17 contributes to non-small cell lung cancer progression via suppressing miR-27a-3p expression and p38 signaling pathway. *Cancer Biol Ther*. 2021;22(1):19-29. doi:10.1080/15384047.2020.1836948
10. Lu X, Kang N, Ling X, Pan M, Du W, Gao S. MiR-27a-3p promotes non-small cell lung cancer through SLC7A11-mediated-ferroptosis. *Front Oncol*. 2021;11:759346. doi:10.3389/fonc.2021.759346
11. Zhao G, Yu H, Ding L, et al. microRNA-27a-3p delivered by extracellular vesicles from glioblastoma cells induces M2 macrophage polarization via the EZH1/KDM3A/CTGF axis. *Cell Death Discov*. 2022;8(1):260. doi:10.1038/s41420-022-01035-z
12. Ku HC, Cheng CF. Master regulator activating transcription factor 3 (ATF3) in metabolic homeostasis and cancer. *Front Endocrinol (Lausanne)*. 2020;11:556. doi:10.3389/fendo.2020.00556
13. Liu H, Kuang X, Zhang Y, et al. ADORA1 inhibition promotes tumor immune evasion by regulating the ATF3-PD-L1 axis. *Cancer Cell*. 2020;37(3):324-339.e8. doi:10.1016/j.ccell.2020.02.006
14. Kumari A, Silakari O, Singh RK. Recent advances in colony stimulating factor-1 receptor/c-FMS as an emerging target for various therapeutic implications. *Biomed Pharmacother*. 2018;103:662-679. doi:10.1016/j.biopha.2018.04.046
15. Wang Y, Lyu Z, Qin Y, et al. FOXO1 promotes tumor progression by increased M2 macrophage infiltration in esophageal squamous cell carcinoma. *Theranostics*. 2020;10(25):11535-11548. doi:10.7150/thno.45261
16. Choe N, Kwon DH, Ryu J, et al. miR-27a-3p targets ATF3 to reduce calcium deposition in vascular smooth muscle cells. *Mol Ther Nucleic Acids*. 2020;22:627-639. doi:10.1016/j.omtn.2020.09.030
17. Li M, Han Y, Wang C, et al. Dissecting super-enhancer driven transcriptional dependencies reveals novel therapeutic strategies and targets for group 3 subtype medulloblastoma. *J Exp Clin Cancer Res*. 2022;41(1):311. doi:10.1186/s13046-022-02506-y
18. Larionova I, Tuguzbaeva G, Ponomaryova A, et al. Tumor-associated macrophages in human breast, colorectal, lung, ovarian and prostate cancers. *Front Oncol*. 2020;10:566511. doi:10.3389/fonc.2020.566511
19. Nielsen MC, Hvidbjerg Gantzel R, Clària J, Trebicka J, Møller HJ, Grønbæk H. Macrophage activation markers, CD163 and

CD206, in acute-on-chronic liver failure. *Cell*. 2020;9(5):1175. doi:10.3390/cells9051175
20. Zhao W, Sun M, Li S, Chen Z, Geng D. Transcription factor ATF3 mediates the radioresistance of breast cancer. *J Cell Mol Med*. 2018;22(10):4664-4675. doi:10.1111/jcmm.13688
21. Kumar V, Donthireddy L, Marvel D, et al. Cancer-associated fibroblasts neutralize the anti-tumor effect of CSF1 receptor blockade by inducing PMN-MDSC infiltration of tumors. *Cancer Cell*. 2017;32(5):654-668.e5. doi:10.1016/j.ccell.2017.10.005
22. Sha H, Zhang D, Zhang Y, Wen Y, Wang Y. ATF3 promotes migration and M1/M2 polarization of macrophages by activating tenascin-C via Wnt/β-catenin pathway. *Mol Med Rep*. 2017;16(3):3641-3647. doi:10.3892/mmr.2017.6992
23. Lin W, Xu D, Austin CD, et al. Function of CSF1 and IL34 in macrophage homeostasis, inflammation, and cancer. *Front Immunol*. 2019;10:2019. doi:10.3389/fimmu.2019.02019
24. Lu CS, Shiau AL, Su BH, et al. Oct4 promotes M2 macrophage polarization through upregulation of macrophage colony-stimulating factor in lung cancer. *J Hematol Oncol*. 2020;13(1):62. doi:10.1186/s13045-020-00887-1
25. Zhu Y, Yang J, Xu D, et al. Disruption of tumour-associated macrophage trafficking by the osteopontin-induced colony-stimulating factor-1 signalling sensitises hepatocellular carcinoma to anti-PD-L1 blockade. *Gut*. 2019;68(9):1653-1666. doi:10.1136/gutjnl-2019-318419
26. Renthal W, Tochitsky I, Yang L, et al. Transcriptional reprogramming of distinct peripheral sensory neuron subtypes after axonal injury. *Neuron*. 2020;108(1):128-144.e9. doi:10.1016/j.neuron.2020.07.026
27. de Sousa VJ, Alawi KM, Keringer P, et al. Examining the role of transient receptor potential canonical 5 (TRPC5) in osteoarthritis. *Osteoarthr Cartil Open*. 2020;2(4):100119.
28. Fu Y, Zhao S, Zhu B, Guo S, Wang X. MiRNA-27a-3p promotes osteogenic differentiation of human mesenchymal stem cells through targeting ATF3. *Eur Rev Med Pharmacol Sci*. 2019;23(3 Suppl):73-80.
29. Xiao M, Yang S, Zhou A, et al. MiR-27a-3p and miR-30b-5p inhibited-vitamin D receptor involved in the progression of tuberculosis. *Front Microbiol*. 2022;13:1020542. doi:10.3389/fmicb.2022.1020542
30. Lee YS, Dutta A. MicroRNAs in cancer. *Annu Rev Pathol*. 2009;4:199-227. doi:10.1146/annurev.pathol.4.110807.092222
31. Mishra S, Yadav T, Rani V. Exploring miRNA based approaches in cancer diagnostics and therapeutics. *Crit Rev Oncol Hematol*. 2016;98:12-23. doi:10.1016/j.critrevonc.2015.10.003
32. Li D, Yan M, Sun F, et al. miR-498 inhibits autophagy and M2-like polarization of tumor-associated macrophages in esophageal cancer via MDM2/ATF3. *Epigenomics*. 2021;13(13):1013-1030. doi:10.2217/epi-2020-0341
33. Sánchez-González I, Bobien A, Molnar C, et al. miR-149 suppresses breast cancer metastasis by blocking paracrine interactions with macrophages. *Cancer Res*. 2020;80(6):1330-1341. doi:10.1158/0008-5472.Can-19-1934

SUPPORTING INFORMATION

Additional supporting information can be found online in the Supporting Information section at the end of this article.

How to cite this article: Zhou B, Xu Y, Xu L, et al. Inhibition of inflammation and infiltration of M2 macrophages in NSCLC through the ATF3/CSF1 axis: Role of miR-27a-3p. *Int J Exp Path*. 2023;104:292-303. doi:10.1111/iep.12490